

Spectral Red-Shift Versus Broadening from Photon and Dilepton Spectra

Jan-e Alam^{1,3}, Pradip Roy², Sourav Sarkar³ and Bikash Sinha^{2,3}

¹ *Physics Department, University of Tokyo, Tokyo 113-0033, Japan*

² *Saha Institute of Nuclear Physics, 1/AF Bidhannagar, Kolkata 700064*

³ *Variable Energy Cyclotron Centre, 1/AF Bidhannagar, Kolkata 700064*

We estimate the photon and dilepton emission rates from hot hadronic matter with in-medium spectral shift and broadening of vector mesons. It is observed that both the WA98 photon data and CERES/NA45 dilepton data can be well reproduced with similar initial conditions. The freeze-out condition has been constrained by the transverse mass spectra of pions and protons measured by the NA49 collaboration. We argue that simultaneous measurement of the p_T spectra of single photons as well as invariant mass distribution of dileptons is crucial to understand the in-medium spectral function of the vector mesons.

PACS: 25.75.+r;12.40.Yx;21.65.+f;13.85.Qk

1. INTRODUCTION

The study of the behaviour of hadrons at finite temperature and/or high baryon density has attracted substantial theoretical and experimental attention in recent times. The theoretical motivation stems from the expectation that broken chiral symmetry of QCD might be restored at high temperature and/or density, at least partially, and this has nontrivial effects on the spectra of low lying hadronic states. Again, these studies are of considerable importance in connection with the experimental detection and study of quark gluon plasma (QGP) in the ultra-relativistic collisions of heavy ions. This is because disentangling the signals from quark matter would require a precise estimate of emissions from hadronic sources which constitutes an overwhelming background in such experiments. Now, the properties of short-lived resonances like the ρ and ω mesons which are likely to decay within the fireball can only be studied through deep probes such as photons and lepton pairs which are essentially electromagnetically interacting and thus probe the entire space-time volume of the collision [1]. The medium modifications of low mass vector mesons has been the subject of numerous theoretical investigations culminating broadly into the following two types of predictions. QCD based models predict a downward shift in the mass, which we will mention as spectral red-shift and a rescattering scenario giving rise to an enhanced width which we have denoted by spectral broadening, the mass remaining largely unchanged. Our aim in this work is to calculate the electromagnetic spectra considering various plausible scenarios and compare with the WA98 [2] photon and CERES/NA45 [3] dilepton spectra in order to comment on the relative importance of the two scenarios

mentioned above.

Our analysis will proceed as follows. In the next section we will define the effective mass and width that have been used in the calculation and define the scenarios of medium effects considered. At the onset we emphasize that our main objective is to see the effect of these contrasting scenarios on the electromagnetic spectra and not on the details of how the forms of the effective mass and the width have been arrived at. Consequently, we will use phenomenological arguments to justify our choice of the parametrisations for these quantities. In section 3 we will discuss the initial conditions in considerable detail. In the relevant transverse momentum region of the photon spectra the main sources of photons are the hard pQCD processes as well as the thermal emissions. Consequently, the number of participants as well as the initial temperature are the relevant initial conditions which have been estimated. For the low mass dilepton spectra, the contribution from Dalitz decays as well as thermal emissions are important. Since photons and dileptons are emitted at all stages of the collision, the space-time evolution plays a very significant role in estimating the total yield. We have used two different approaches to study this aspect; relativistic hydrodynamics and transport. As we shall see, medium effects do play a very important role in the equation of state and consequently the cooling profile. These aspects have been dealt with in section 4. The transverse mass (m_T) spectra of pions and protons obtained at SPS have been evaluated and compared with data from NA49 [4] in section 5 in order to estimate the freeze-out condition which goes as an input into the hydrodynamic calculations. With all these inputs we evaluate the photon and dilepton spectra in sections 6 and 7 respectively. section 8 contains a summary and discussions.

2. EFFECTIVE MASS AND WIDTH OF HADRONS

It has been emphasized that the properties of hadrons will be modified due to its interaction with the particles in the thermal bath and such modifications will be reflected in the dilepton and photon spectra emitted from the system (see Refs. [5–9] for review). Broadly two types of medium modifications are expected: shift in the pole position and/or broadening of the spectral function. As discussed earlier, our main objective is to comment on the nature of medium effects through the study of WA98

photon and CERES dilepton data. Accordingly we consider the following scenarios: (I) the system is formed in the hadronic phase with the hadronic masses (except pseudoscalars) approaching zero near the critical temperature according to the universal scaling law [5,10]. The in-medium masses of the hadrons and the decay width of ρ are taken as

$$m_H^*/m_H = (1 - T^2/T_c^2)^\lambda$$

$$\Gamma_\rho = \frac{g_{\rho\pi\pi}^2}{48\pi} m_\rho^* (1 - 4m_\pi^2/m_\rho^{*2})^{3/2} (1 + 2f_{BE}) \quad (1)$$

where f_{BE} is the Bose-Einstein distribution. For the width of ω see Ref. [9]. (II) the width of the vector meson (ρ) increasing with temperature as,

$$\Gamma_\rho^* = \Gamma_\rho / (1 - T^2/T_c^2),$$

$$m_H^* = m_H \quad (2)$$

and the masses remain constant at their vacuum values. The value of λ in eq. 1 is 1/6 and 1/2 for Brown-Rho and Nambu scaling [5] respectively. The present experimental statistics can not differentiate among different values of λ . Therefore, we leave it as a parameter here. The scenario II derives motivation from the results of chiral models according to which the mass of the ρ does not change to order T^2 but the leading order T -dependence of the pion decay constant results in the ρ decay width having the form described by Eq. 2. We have also considered a third case, (III) in which both the masses and widths are maintained at the vacuum values. In eqs. 1 and 2, T_c is the critical temperature of chiral symmetry restoration where the quark condensate $\langle \bar{q}q \rangle$ and consequently the mass of the hadrons tend to zero.

Let us study the in-medium effects on the thermal phase space factor through the ρ meson as it plays the most important role for the electromagnetic probes. In Fig. 1 we display the change in the density of thermal ρ as a function of temperature for scenarios (I), (II) and (III) by solid, dotted and long-dashed lines respectively. It is clear that the density of ρ is very sensitive to the spectral shift of ρ mass due to Boltzmann enhancement but rather insensitive to the change of width. The reason for small change in the density of ρ due to the in-medium broadening can be understood from the following arguments. The density of an unstable vector meson (say, ρ) in a thermal bath can be written as [11],

$$\frac{dN}{d^3k d^3x ds} = \frac{g}{(2\pi)^3} \frac{1}{e^{\sqrt{k^2+s}/T} - 1} P(s) \quad (3)$$

where g is the statistical degeneracy of the particle and $P(s)$ is the spectral function,

$$P(s) = \frac{1}{\pi} \frac{\text{Im } \Pi}{(s - m_\rho^2 - \text{Re } \Pi)^2 + (\text{Im } \Pi)^2} \quad (4)$$

$\text{Im } \Pi$ ($\text{Re } \Pi$) is the imaginary (real) part of the ρ self energy. Eqs. 3 and 4 indicate that the density of particles (vector mesons) in a thermal bath is given by the

Bose-Einstein distribution weighted by the Breit-Wigner function, which gets maximum weight from the value of $s = m_\rho^2 + \text{Re } \Pi$, the contribution from either side of the maximum being averaged out. Therefore, the results become sensitive to the value of $s = m_\rho^{2*} = m_\rho^2 + \text{Re } \Pi$ and not to the width of the spectral distribution. Note that $P(s)$ tends to $\delta(s - m_\rho^2 - \text{Re } \Pi)$ as $\text{Im } \Pi \rightarrow 0$, corresponding to a stable particle. (Here, Π is proportional to the trace of the self energy tensor $\Pi_{\mu\nu}$ of the ρ).

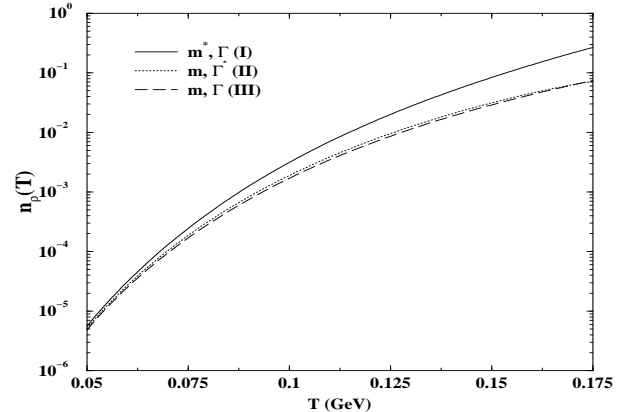


FIG. 1. Solid (long dashed) line represent density of thermal ρ as a function of temperature with in-medium mass and vacuum width (vacuum mass and width). Dotted line represents the density with vacuum mass and in-medium width.

3. INITIAL CONDITIONS

Here we will discuss the parameters which enter as inputs to the evaluation of electromagnetic and hadronic spectra from relativistic heavy ion collisions corresponding to different scenarios considered. We begin with the quantity $n(b)$ which is the average number of nucleon-nucleon collisions in the collision of two nuclei of mass numbers A and B at an impact parameter b . This is given by [12],

$$n(b) = AB T_{AB}(b) \sigma_{in} \quad (5)$$

where $T_{AB}(b)$ is the nuclear overlap integral evaluated from the following expression,

$$T_{AB}(\vec{b}) = \int d^2s T_A(\vec{s}) T_B(\vec{b} - \vec{s}), \quad (6)$$

and the thickness function, T_A is defined as $T_A(\vec{b}) = \int dz \rho_A(\vec{b}, z)$. The nuclear density, $\rho_A(\vec{b}, z)$ is parametrized by Wood-Saxon type profile function [13],

$$\rho_A(r) = \rho_0 \frac{1 + \omega r^2/R_A^2}{1 + e^{(r-R_A)/z}} \quad (7)$$

where $\omega = 0$, $z = 0.549$ for the Pb nucleus and $R_A = 1.2A^{1/3}$ and the central density, ρ_0 is determined by the normalization condition $\int d^3r \rho_A(r) = 1$. In Fig. 2 $n(b)$

is shown as a function of the impact parameter, b . The most central event in WA98 corresponds to $b \sim 3.2$ fm/c. At this value of the impact parameter $n(b) \sim 660$.

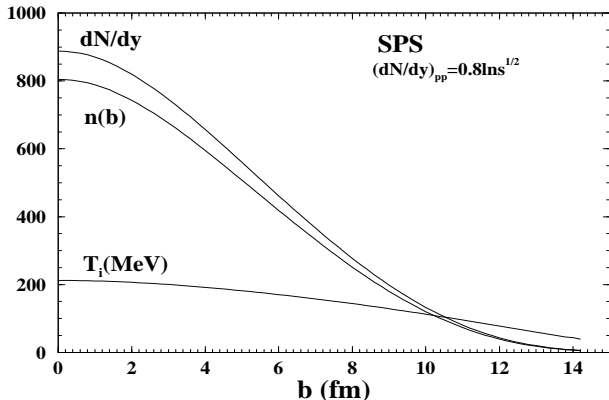


FIG. 2. Hadron multiplicity, effective number of nucleon-nucleon collisions and initial temperature as a function of impact parameter calculated by using Glauber model for nucleus - nucleus collisions (see text).

The hadron multiplicity in A + B collisions at an impact parameter b can then be evaluated in terms of the multiplicity in pp collisions as [12],

$$\frac{dN}{dy}(b) = \frac{n(b)}{1 + \delta(A^{1/3} + B^{1/3})} \frac{dN_{pp}}{dy}, \quad (8)$$

where $dN_{pp}/dy = 0.8 \ln \sqrt{s}$ is the hadron multiplicity for nucleon-nucleon collisions at mid-rapidity [14]. The value of dN/dy is 725 at $b \sim 3.2$ fm, $\sqrt{s} = 17.3$ GeV and $\delta = 0.09$ (see Fig.2). The term $1 + \delta(A^{1/3} + B^{1/3})$ takes into account the energy degradation of the participating nucleons in the nuclear environment. For isentropic expansion the initial temperature (T_i) is related to the hadron multiplicity as,

$$T_i^3(b) = \frac{2\pi^4}{45\xi(3)} \frac{1}{\pi R_A^2 \tau_i 4a_k} \frac{dN}{dy}(b) \quad (9)$$

$a_k = \pi^2 g_k/90$ is determined by the statistical degeneracy (g_k) of the system formed after the collision. In case of a deconfined initial state, $g_k = 37$ considering a non-interacting gas of gluons and quarks of two flavours. For a hadron gas composed of π , ρ , ω , η , a_1 and nucleons the effective degeneracy has a value ~ 30 near the critical temperature where the hadronic masses go to zero according to the universal scaling scenario [5]. The increase in the degeneracy originates from the heavier hadrons going to a massless situation (see also [15]). A value of $g_{eff} \sim 30$ can also be realized from the lattice data [16,17] near the phase transition point by using the relation $s/T^3 = 4\pi^2 g_{eff}/90$, where s is the entropy density. The latter is calculated using the relation, $s = (\epsilon + P)/T$ and contains the effect of the in-medium masses of the constituent hadrons (for details see [9]).

For $\tau_i = 1$ fm/c [18] and $g_k \sim 30$, we get an initial temperature $T_i(b \sim 3.2$ fm) ~ 200 MeV (see Fig. 2). Note that the variation of $T_i(b)$ as a function of the impact parameter is very slow because $T_i(b) \sim [dN/dy(b)]^{1/3}$. In an attempt to understand the lattice data in terms of the effective fields [19] the effective degrees of freedom in hadrons was limited to ~ 24 which coincides with the number of fundamental degrees of freedom for two quark flavors.

4. SPACE-TIME EVOLUTION AND EQUATION OF STATE

Next we study the sensitivity of the results on the space-time evolution. In order to do that we solve the (3+1) dimensional hydrodynamic equations with initial energy density [20],

$$\epsilon(\tau_i, r) = \frac{\epsilon_0}{e^{(r-R_A)/\delta} + 1} \quad (10)$$

and initial velocity profile, $v_r = v_0(r/R_A)^\alpha$ which has been successfully used to study transverse momentum spectra of hadrons [21,22] and photons [23–25]. For our numerical calculations we choose $\alpha = 1$ and $v_0 = 0$ at the initial time.

The equation of state (EOS) used here to solve the hydrodynamic equations is evaluated as in Ref. [9]. The temperature dependence of the mass enters into the EOS through the effective statistical degeneracy (g_{eff}). In Fig. 3 the temperature variation of the effective degeneracy obtained from different models for the hadronic interactions (see [9] for details) is compared with the lattice QCD calculations [26]. The co-efficient of ϵ/T^4 differs from the effective degeneracy by a factor of $\pi^2/30$. The lattice data seems to be well reproduced by the universal scaling scenario of mass reduction given by eq. 1. In this case the velocity of sound (c_s) is given by $c_s^{-2} = T ds/sdT = [(T/g_{eff})(dg_{eff}/dT) + 3]$ [27]. Clearly, the value of c_s is less than its value corresponding to ideal fluid case ($c_s^{ideal} = 1/\sqrt{3}$). This affects the space time evolution of the system non-trivially. In solving the hydrodynamic equations we have used the equation of state which contains the in-medium shift of the hadronic spectral functions as described above.

The integration over the space time history has also been performed by taking the temperature profile from the transport model where the temperature varies with time as follows:

$$T(t) = (T_i - T_\infty)e^{-t/\tau} + T_\infty \quad (11)$$

The cooling law given above is the parametrization of the results of [28], used in several articles in the literature [29] (see also the review [8] and references therein). The calculation is performed with the following values of parameters: $T_i = 200$ MeV, $T_\infty = 120$ MeV, $\tau = 8$ fm/c.

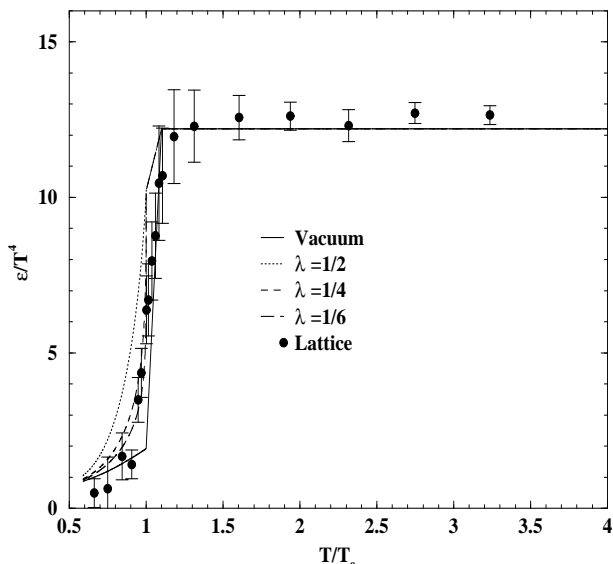


FIG. 3. The energy density ϵ in the unit of T^4 for the equation of state for various models of hadronic interactions is plotted as function of temperature (T) in the unit of the critical temperature, T_c . The filled circle denotes the lattice results [26]. The universal scaling scenario seems to describe the lattice results quite well near the T_c . For $T > T_c$ the bag model equation of state has been used.

5. HADRONIC SPECTRA AND FREEZE-OUT TEMPERATURE

Having fixed the initial temperature and the equation of state we now need to fix another important parameter, the freeze-out temperature T_F where the hydrodynamic evolution should terminate. At this stage the mean free path of the constituents begin to exceed the size of the system and particles start free streaming to the detector. For this purpose we will consider the $m_T (= \sqrt{p_T^2 + m^2})$ spectra [30,31] of pions and protons measured in Pb + Pb collisions at SPS energies by the NA49 collaboration [4]. We will assume that pions and nucleons are in thermal equilibrium throughout the evolution until they freeze-out at a common temperature T_F . Negative hadrons and positive minus the negative are treated as pions and protons respectively. The π^- and K^- from the decays ρ and ϕ are about 5% of the direct pions at $p_T \sim 500$ MeV and are therefore neglected here. In fig. 4 NA49 pion spectra is compared with the hadronic initial states with $T_i \sim 200$ MeV and $T_F = 100, 120$ and 140 MeV. We find a reasonable agreement for $T_F = 120$ MeV as far as the slope is concerned. Calculations are done with all the scenarios I, II and III. Due to reasons explained in section 2, the results with scenario II are indistinguishable from that of scenario III. We arrive at similar conclusions from the analysis of the proton spectra as shown in fig. 5.

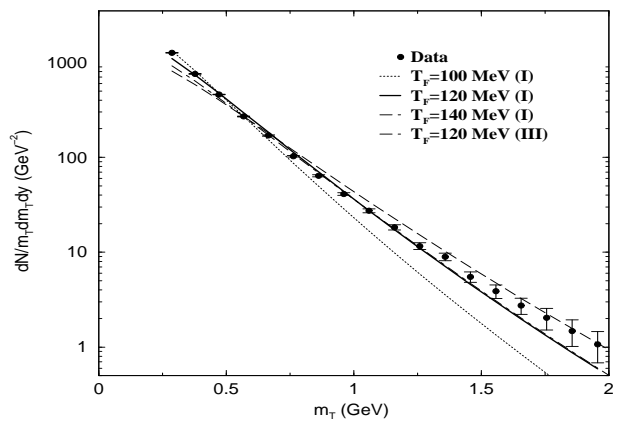


FIG. 4. The m_T distribution of pions for Pb + Pb collisions at CERN SPS energies.

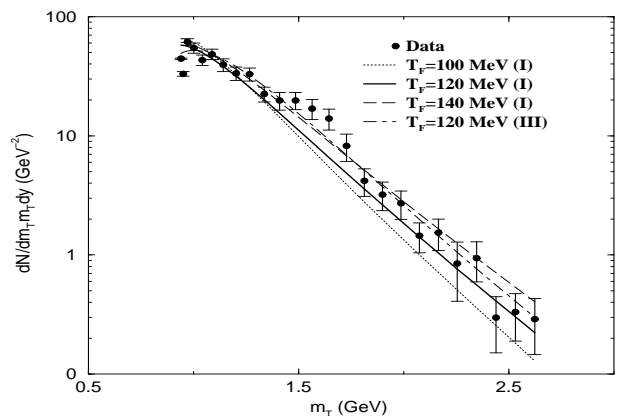


FIG. 5. The m_T distribution of protons for Pb + Pb collisions at CERN SPS energies.

6. PHOTON SPECTRA

We start with the single photon data of WA98 collaboration which has initiated considerable theoretical activities [23–25,32–34]. For the analysis of WA98 photon spectra, we consider prompt photons resulting from the hard collisions of the partons in the colliding nuclei and the thermal photons from a hot hadronic gas with possible in-medium modifications. Photons from hadronic decays ($\pi^0 \rightarrow \gamma\gamma$, $\eta \rightarrow \gamma\gamma$ etc.) are already subtracted from the data [2] and hence we need not consider them here. We begin our discussions with the prompt photon. The prompt photon yield for nucleus-nucleus collision is given by,

$$E \frac{dN}{d^3p} = n(b) \frac{1}{\sigma_{in}} E \frac{d\sigma_{pp}}{d^3p} \quad (12)$$

where $n(b)$ is the average number of nucleon-nucleon collisions at an impact parameter b , and σ_{in} ($=30$ mb, taken from Ref. [2]) is the $p-p$ inelastic cross section. The prompt photon contributions have been evaluated with possible intrinsic transverse motion of the par-

tons [33,35] inside the nucleon and multiplied by a K -factor ~ 2 , to account for the higher order effects. The CTEQ(5M) parton distributions [36] have been used for evaluating hard photons. The relevant value of \sqrt{s} , energy in the centre of mass for WA98 experiment is 17.3 GeV. No experimental data on hard photons exist at this energy. Therefore, the “data” at $\sqrt{s} = 17.3$ GeV is obtained from the data at $\sqrt{s} = 19.4$ GeV of the E704 collaboration [37] by using the scaling relation: $Ed\sigma/d^3p_\gamma|_{h_1+h_2 \rightarrow C+\gamma} = f(x_T = 2p_T/\sqrt{s})/s^2$, for the hadronic process, $h_1 + h_2 \rightarrow C + \gamma$ [38]. This scaling is valid in the naive parton model. However, such scaling may be spoiled in perturbative QCD due to the reasons, among others, the momentum dependence of the strong coupling, α_s and from the scaling violation of structure functions, resulting in faster decrease of the cross section than $1/s^2$ [35]. Therefore, the data at $\sqrt{s} = 17.3$ GeV obtained by using the above scaling gives a conservative estimate of the prompt photon contributions. We have seen that the effects of the nuclear shadowing in parton distributions on the prompt photons are negligibly small at SPS but it is important at RHIC and LHC energies [39]. This is because the value of $x(\sim 2p_T/\sqrt{s})$ at SPS is not small enough for the shadowing effects to be important.

To evaluate the photon emission rate from a hadronic gas we model the system as consisting of π , ρ , ω η and a_1 [40,41]. The relevant vertices for the reactions $\pi\pi \rightarrow \rho\gamma$ and $\pi\rho \rightarrow \pi\gamma$ and the decay $\rho \rightarrow \pi\pi\gamma$ are obtained from the following Lagrangian:

$$\mathcal{L} = -g_{\rho\pi\pi}\vec{\rho}^\mu \cdot (\vec{\pi} \times \partial_\mu \vec{\pi}) - eJ^\mu A_\mu + \frac{e}{2}F^{\mu\nu} (\vec{\rho}_\mu \times \vec{\rho}_\nu)_3, \quad (13)$$

where $F_{\mu\nu} = \partial_\mu A_\nu - \partial_\nu A_\mu$, is the field tensor for electromagnetic field and J^μ is the hadronic part of the electromagnetic current given by

$$J^\mu = (\vec{\rho}_\nu \times \vec{q}^{\nu\mu})_3 + (\vec{\pi} \times (\partial^\mu \vec{\pi} + g_{\rho\pi\pi}\vec{\pi} \times \vec{\rho}^\mu))_3, \quad (14)$$

with $\vec{q}_{\mu\nu} = \partial_\mu \vec{\rho}_\nu - \partial_\nu \vec{\rho}_\mu - g_{\rho\pi\pi}(\vec{\rho}_\mu \times \vec{\rho}_\nu)$. $\vec{\pi}$, $\vec{\rho}^\mu$ and A^μ represent the π , ρ and photon fields respectively and the arrows represent vectors in isospin space. $g_{\rho\pi\pi}$ denotes the coupling strength of the $\rho\pi\pi$ vertex, fixed from the observed decay width $\rho \rightarrow \pi\pi$. We have also considered the photon production due to the reactions $\pi\eta \rightarrow \pi\gamma$, $\pi\pi \rightarrow \eta\gamma$ and the decay $\omega \rightarrow \pi\gamma$ using the interaction given in [42] and vector meson dominance [43]:

$$\mathcal{L} = \frac{g_{\rho\rho\eta}}{m_\eta} \epsilon_{\mu\nu\alpha\beta} \partial^\mu \rho^\nu \partial^\alpha \rho^\beta \eta + \frac{g_{\omega\rho\pi}}{m_\pi} \epsilon_{\mu\nu\alpha\beta} \partial^\mu \omega^\nu \partial^\alpha \rho^\beta \pi + \sum_{V=\rho,\omega} \frac{em_V^2}{g_V} V^\mu A_\mu \quad (15)$$

where $\epsilon_{\mu\nu\alpha\beta}$ is the totally anti-symmetric Levi-Civita tensor. The invariant amplitudes for all the reactions are given in Ref. [41]. The values of $g_{\rho\rho\eta}$ and $g_{\omega\rho\pi}$ are

fixed from the observed decays, $\rho \rightarrow \eta\gamma$ and $\omega \rightarrow \pi\gamma$ respectively. The constant g_V is determined from the decays, $V \rightarrow e^+e^-$. Photon production due to the process $\pi\rho \rightarrow a_1 \rightarrow \pi\gamma$ is also taken into consideration (for details of interaction vertices see [9]).

In Fig. 6 the static (fixed temperature) photon spectra is shown for $T = 180$ MeV. The solid line shows the enhanced yield with in-medium masses and vacuum widths compared to the yield obtained with vacuum masses and widths (dotted line). The long-dashed line showing the result with in-medium width and vacuum masses does not differ substantially from the dotted line, because we find that the effects of the change in the decay width both on the phase space and the production cross section are small. We observe that the contributions from the decays of baryonic resonances ($N(1520)$, $N(1535)$, $N(1440)$, $\Delta(1232)$, and $\Delta(1620)$) are also small (filled circle). The values of the decay widths, $R \rightarrow N\gamma$, where R and N denote the baryonic resonances and the nucleon respectively, are taken from the particle data book [44]. It is observed that the photon yield with universal mass variation scenarios, I is almost an order magnitude larger than the case II with large broadening of the ρ . Reduction in the hadronic masses causes an enhancement in the thermal distribution of mesons because of which the rate of thermal emission of photons increases. The scenario with vacuum values of both masses and width (dotted line) does not show any appreciable difference from (II).

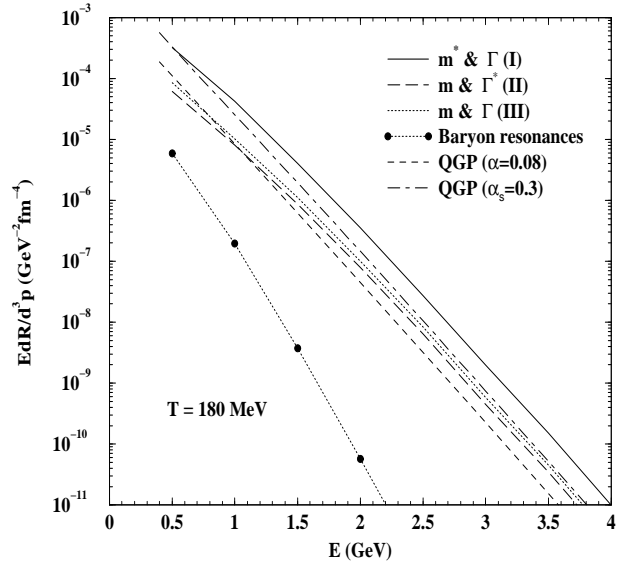


FIG. 6. The photon production rate as function of its energy at a temperature, $T = 180$ MeV. Solid (long dashed) line indicates rate for scenario I (scenario II). Dotted line represents the spectra without any medium effects. Filled circles indicate photons originating from baryonic resonance decays. Short dashed (dot-dashed) line indicates the photon emission rate from a thermalized two-flavor quark gluon plasma for $\alpha_s = 0.08(0.2)$.

For the sake of comparison we have also shown the photon emission rate from a thermalized QGP. The photon spectra from QGP includes Compton, annihilation, bremsstrahlung and annihilation with scattering processes [40,45–47] (see also [48]). Here we have mainly focused on photon production from hot hadronic matter and hence do not consider emission rate from QGP beyond two loops [49]. From the lattice results [50] the value of $\alpha_s \sim 0.3 (g^2 = 4)$ at $T = 180$ MeV. At $T = 180$ MeV the emission rates from the QGP (dot-dashed) and hot hadronic matter (scenario II and III) are comparable for $p_T > 1.5$ GeV. The photon yield from hadronic matter for scenario I is substantially larger than that from QGP. However, it should be mentioned here that the photon emission rate from QGP is evaluated in Refs. [40,45,46] by using hard thermal loop (HTL) approximations, which is valid for the value of the color charge, $g \ll 1$. The validity of the HTL approximation to higher values of g is doubtful. In fact, such an extrapolation in the value of g (from $g \ll 1$ to $g \sim 2$) introduces an uncertainty by a factor of ~ 5 . Due to these uncertainties we must be careful in making any firm conclusion from the results obtained on the basis of the HTL approximations. For $\alpha_s = 0.08 (g = 1)$ the emission rate from QGP (short-dashed line) is much smaller than the rates from hadronic matter.

In Fig. 7 the p_T distribution of photons (prompt+thermal) is compared with the WA98 data. Within the framework of the transport model the data is well reproduced when the hadronic masses are allowed to vary according to the eqs. 1 (long-dash line, scenario I). However, when scenario (II) is considered for thermal photons (dash dotted line) the experimentally observed “excess” photon in the region $1.5 \leq p_T$ (GeV) ≤ 2.5 is not reproduced. The dotted line indicates results with vacuum masses and widths.

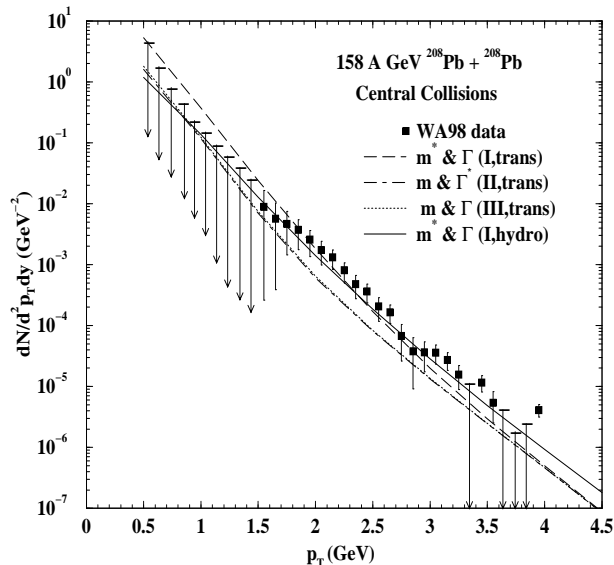


FIG. 7. Total (prompt+thermal) photon yield in Pb + Pb collisions at 158 A GeV at CERN-SPS. The theoretical calculations contain hard QCD and thermal photons. The system is formed in the hadronic phase with initial temperature $T_i = 200$ MeV; ‘trans’ indicates the results for the cooling law 11.

The photon yield for the scenario (I) shown in Fig. 7 (solid line) is obtained by folding the static rate with the space time history of the system governed by relativistic hydrodynamics from the initial to the freeze-out state (freeze-out temperature ~ 120 MeV); the data is well reproduced in this case also.

The agreement between the p_T spectra of photon obtained with two different types of space time evolution scenarios (transport model and hydrodynamics) can be explained as follows. We find that the variation of temperature with time (cooling law) in eq. 11 is slower than the one obtained by solving hydrodynamic equations. As a consequence the thermal system has a longer life time than the former case, allowing the system to emit photons for a longer time. In case of hydrodynamics this is compensated by the transverse kick due to radial velocity of the expanding matter which shifts some of the photon multiplicity from lower values of transverse momentum towards the higher region.

7. DILEPTON SPECTRA

Now we study the invariant mass distribution of lepton pairs measured by CERES/NA45 collaboration [3] in Pb + Au collisions. We consider the thermal dilepton production in the hadronic medium due to the process $\pi^+\pi^- \rightarrow e^+e^-$, known to be the most dominant source of dilepton production from hadronic matter. In the thermal system the width of the ω meson can be large due to various reactions occurring in the thermal bath, the most dominant process, among others, is $\omega\pi \leftrightarrow \pi\pi$ [9,51]. As a consequence of this, the life time of the ω meson could become smaller compared to the life time of the hadronic system, enabling it to decay in the interior of the system. In view of this the in-medium decay $\omega \rightarrow e^+e^-$ is also taken into account. The required interaction vertices have been obtained from eqs. (13), (14) and (15). In Fig. 8 the experimental data is compared with the theoretical results for $dN_{ch}/d\eta = 270$. The effective masses and widths of ρ and ω mesons appearing in the processes $\pi\pi \rightarrow \rho \rightarrow e^+e^-$ and $\omega \rightarrow e^+e^-$ respectively are taken from Eq. 1 (for details on the thermal emission rate of lepton pairs see Ref. [9]). Contributions from hadronic decays at freeze-out (background) is taken from the second of Ref. [3] (dotted line). The observed enhancement of the dilepton yield around $M \sim 0.3 - 0.6$ GeV can be reproduced by the scenarios (I) (long-dashed) and (II) (dot-dashed) when the cooling law is taken as eq. 11. The data is also well reproduced when hydrodynamics is used to describe the space time evolution of the system

for the scenario I (solid line). However, with vacuum properties of the vector mesons the low mass enhancement can not be reproduced (short-dashed), indicating the change of vector meson properties in the medium. It is interesting to recall here that in a recent experiment Ozawa *et al* [52] has observed a significant enhancement in the dilepton yield in p + Cu collisions as compared to p + C collisions below the ω peak.

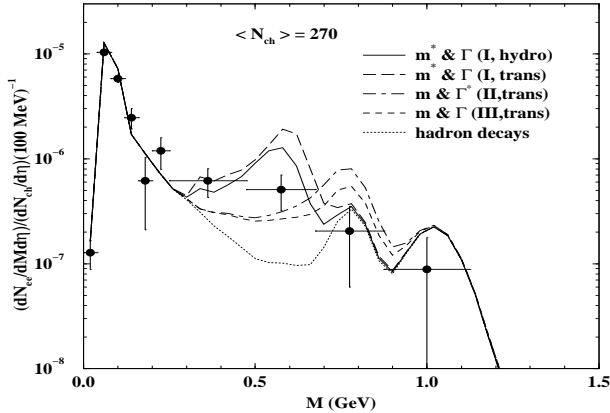


FIG. 8. Dilepton spectra for $\langle N_{ch} \rangle = 270$ for different scenarios as indicated in the text.

8. SUMMARY AND DISCUSSIONS

Let us now summarise the results. We reiterate that our main contention in this work is to comment on the nature of medium effects vis-a-vis mass shift as opposed to broadening of the spectral density of hadrons. Such a study is only possible through the electromagnetic probes since they are sensitive to the evolution of the spectral function of vector mesons. The freeze-out conditions within the model used for evaluating the photon and dilepton spectra have been estimated through the NA49 pion and proton spectra. Firstly, we find that the WA98 photon transverse momentum spectra and the CERES dilepton low invariant mass spectra is well explained if we assume a chirally restored initial phase at a temperature ~ 200 MeV where the masses of the hadrons tend to zero and grow to their vacuum values with the decrease of temperature. In fact, close to the critical temperature for chiral symmetry restoration (in our case $\sim T_i = 200$ MeV) the description of the system either in terms of partonic or hadronic degrees of freedom become dual, although the non-perturbative effects may still be important. For example, the emission rate of dileptons from pion annihilation will resemble that from $q\bar{q}$ annihilation, because of the complete extinction of the intermediary ρ at the critical temperature [8,9]. This indicates that the $q\bar{q}$ interaction in the vector channel has become weak, signalling the onset of chiral transition. Whether such a state is synonymous with deconfined matter (QGP) is still an unsettled issue. A similar value of the initial temperature is obtained in Refs. [24,25,27,53]. Based on

the present and our earlier results [24], it is fair to say that a simple hadronic model with vacuum properties of hadrons is inadequate to explain the above experimental data. Either a substantial change in the in-medium hadronic spectral function or the formation of the QGP is required. More importantly, we find that the p_T distribution of photons changes significantly with a reduced mass scenario and is almost unaffected by the broadening of the vector meson spectral function in the medium. The invariant mass distribution of the lepton pairs on the other hand can be explained with both a reduction in the mass as well as with an enhanced width of the vector mesons. Thus by looking only at the dilepton spectra it is difficult to differentiate the above scenarios; we need to analyse both the photon and dilepton spectra simultaneously. With better statistics we might succeed in ruling out or at least restricting one of the scenarios. We expect that such a situation should be realized at the Relativistic Heavy Ion Collider (RHIC).

Acknowledgement: We are grateful to Tetsuo Hatsuda for useful comments on this manuscript. Useful discussions with Tapan K. Nayak is thankfully acknowledged. J.A. is grateful to the Japan Society for Promotion of Science (JSPS) for financial support. J.A. is also supported by Grant-in-aid for Scientific Research No. 98360 of JSPS.

-
- [1] L. McLerran and T. Toimela, Phys. Rev. **D 31**, 545 (1985); C. Gale and J. I. Kapusta, Nucl. Phys. **B357**, 65 (1991); E. V. Shuryak, Phys. Rep. **61**, 71 (1980); J. Alam, S. Raha and B. Sinha, Phys. Rep. **273**, 243 (1996); W. Cassing and E. L. Bratkovskaya, Phys. Rep., **308**, 65 (1999).
 - [2] M. M. Aggarwal *et al.*, WA98 Collaboration, Phys. Rev. Lett. **85**, 3595 (2000).
 - [3] G. Agakichiev *et al.*, CERES Collaboration, Phys. Lett. **B 422**, 405 (1998); B. Lenkeit, Doctoral Thesis, Universitaet Heidelberg (1998).
 - [4] H. Appelshäuser *et al.*, NA49 Collaboration, Phys. Rev. Lett. **82**, 2471 (1999).
 - [5] G. E. Brown and M. Rho, Phys. Rep. **269**, 333 (1996); Phys. Rep. **363**, 85 (2002).
 - [6] T. Hatsuda and T. Kunihiro, Phys. Rep. **247**, 221 (1994).
 - [7] R. D. Pisarski, hep-ph/9503330.
 - [8] R. Rapp and J. Wambach, Adv. Nucl. Phys. **25**, 1 (2000).
 - [9] J. Alam, S. Sarkar, P. Roy, T. Hatsuda and B. Sinha, Ann. Phys.(NY), **286**, 159 (2000).
 - [10] G. E. Brown and M. Rho, Phys. Rev. Lett. **66**, 2720(1991).
 - [11] H. A. Weldon, Ann. Phys. (NY) **228**, 43 (1993).
 - [12] C. Y. Wong, Introduction to high energy heavy ion collisions, World Scientific, Singapore, 1994.
 - [13] K. J. Eskola, R. Vogt and X. N. Wang, Int. J. Mod. Phys. A **10**, 3087 (1995).

- [14] U. Heinz, P. Koch and B. Friman, in Proc. Large Hadron Collider Workshop, Aachen, 1990, CERN-90-10, Vol. II, p. 1079.
- [15] V. Koch and G. E. Brown, Nucl. Phys. **A 560**, 345 (1993).
- [16] F. Karsch, hep-ph/0103314.
- [17] M. Asakawa and T. Hatsuda, Phys. Rev. **D55**, 4488 (1997).
- [18] J. D. Bjorken, Phys. Rev. **D27**, 140 (1983).
- [19] G. E. Brown, H. A. Bethe, A. D. Jackson and P. M. Pizzochero, Nucl. Phys. **A 560**, 1035 (1993).
- [20] H. von Gersdorff, M. Kataja, L. McLerran and P. V. Ruuskanen, Phys. Rev. **D 34**, 794 (1986).
- [21] P. Braun-Munzinger, J. Stachel, J. P. Wessels and N. Xu, Phys. Lett. **B 365**, 1 (1996).
- [22] U. Heinz, K. S. Lee and E. Schnedermann, in Quark Gluon Plasma, edited by R. C. Hwa, (World Scientific, Singapore 1992); J. Alam, J. Cleymans, K. Redlich and H. Satz, nucl-th/9707042.
- [23] K. Gallmeister, B. Kämpfer and O. P. Pavlenko, Phys. Rev. **C 62**, 057901 (2000).
- [24] J. Alam, S. Sarkar, T. Hatsuda, T. K. Nayak and B. Sinha, Phys. Rev. **C 63**, 021901R (2001).
- [25] D. Yu. Peressounko and Yu. E. Pokrovsky, hep-ph/0009025.
- [26] F. Karsch, hep-lat/0106019.
- [27] S. Sarkar, J. Alam and T. Hatsuda, nucl-th/0011032.
- [28] G. Q. Li, C. M. Ko, G. E. Brown, Phys. Rev. Lett. **75**, 4007 (1995); Nucl. Phys. **A 606**, 568 (1996).
- [29] R. Rapp, G. Chanfray and J. Wambach, Phys. Rev. Lett. **76**, 368 (1996); Nucl. Phys. **A 617**, 472 (1997).
- [30] P. V. Ruuskanen, Acta Phys. Pol. **A 18**, 551 (1986).
- [31] J. P. Blaizot and J. Y. Ollitrault, in Quark Gluon Plasma, edited by R. C. Hwa, (World Scientific, Singapore 1992).
- [32] S. Sarkar, P. Roy, J. Alam and B. Sinha, Phys. Rev. **C 60**, 054907 (1999).
- [33] C. Y. Wong and H. Wang, Phys. Rev. **C 58**, 376 (1998).
- [34] D. K. Srivastava and B. Sinha, Phys. Rev. **C 64** 034902 (2001).
- [35] J. F. Owens, Rev. Mod. Phys. **59**, 465 (1987).
- [36] H. L. Lai, et. al., Eur. Phys. J. **C 12**, 375 (2000).
- [37] E704 Collaboration, D. L. Adams et al, Phys. Lett. **B 345**, 569 (1995).
- [38] T. Ferbel and W. R. Molzon, Rev. Mod. Phys. **56**, 181 (1984).
- [39] P. Roy et. al. to be published.
- [40] J. I. Kapusta, P. Lichard, and D. Seibert, Phys. Rev. **D44**, 2774 (1991).
- [41] S. Sarkar, J. Alam, P. Roy, A. K. Dutt-Mazumder, B. Dutta-Roy and B. Sinha, Nucl. Phys. **A634**, 206 (1998); P. Roy, S. Sarkar, J. Alam and B. Sinha, Nucl. Phys. **A 653**, 277 (1999).
- [42] M. Gell-Mann, D. Sharp and W. D. Wagner, Phys. Rev. Lett. **8**, 261 (1962).
- [43] J. J. Sakurai, Currents and Mesons, The University of Chicago Press, Chicago, 1969.
- [44] Particle Data Group, R. M. Barnett *et. al.*, Phys. Rev. **D 54**, 1 (1996).
- [45] Baier, H. Nakkagawa, A. Niegawa and K. Redlich, Z. Phys. **C53**, 433 (1992).
- [46] P. Aurenche, F. Gelis, H. Zaraket and R. Kobes, Phys. Rev. **D 58**, 085003 (1998).
- [47] F. D. Steffen and M. H. Thoma, Phys. Lett. **510**, 98 (2001).
- [48] D. Dutta, S. V. S. Sastry, A. K. Mohanty, K. Kumar and R. K. Choudhury, Nucl. Phys. **A 710**, 415 (2002).
- [49] The thermal photon emission rate from QGP complete to order α_s has recently been obtained in [54] which was used by Huovinen et. al. [55] to analyze the WA98 photon data).
- [50] F. Karsch, Z. Phys. **C38** 147 (1988).
- [51] J. Alam, S. Sarkar, P. Roy, B. Dutta-Roy and B. Sinha, Phys. Rev. **C59**, 905 (1999).
- [52] K. Ozawa *et al*, Phys. Rev. Lett. **86** 5019 (2001).
- [53] R. Rapp E. Shuryak, Phys. Lett. **B 473**, 13 (2000); K. Gallmeister, B. Kämpfer and O. P. Pavlenko, Phys. Lett. **B 473**, 20 (2000).
- [54] P. Arnold, G. D. Moore and L. G. Yaffe, Jour. High Enr. Phys. **0111** 057 (2001); *ibid.* **0111** 057 (2001).
- [55] P. Huovinen, P. V. Ruuskanen and S. S. Rasanen, Phys. Lett. **B 535** 109 (2002).